Atmos. Chem. Phys. Discuss., 15, 11277–11323, 2015
www.atmos-chem-phys-discuss.net/15/11277/2015/
doi:10.5194/acpd-15-11277-2015

Atmospheric Chemistry and Physics Discussions

The impact of shipping emissions on air pollution in the Greater North Sea region – Part 1: Current emissions and concentrations

A. Aulinger[1], V. Matthias[1], M. Zeretzke[2], J. Bieser[1], M. Quante[1], and A. Backes[1]

[1]Helmholtz-Zentrum Geesthacht, Institute of Coastal Research, Max-Planck-Straße 1, 21502 Geesthacht, Germany
[2]DNV-GL, Brooktorkai 18, 20457 Hamburg, Germany

Received: 29 January 2015 – Accepted: 21 March 2015 – Published: 16 April 2015

Correspondence to: A. Aulinger (armin.aulinger@hzg.de)

Published by Copernicus Publications on behalf of the European Geosciences Union.

Abstract

The North Sea is one of the areas with the highest ship traffic densities worldwide. At any time, about 3000 ships are sailing its waterways. Previous scientific publications have shown that ships contribute significantly to atmospheric concentrations of NO_x, particulate matter and ozone. Especially in the case of particulate matter and ozone this influence can even be seen in regions far away from the main shipping routes. In order to quantify the effects of North Sea shipping on air quality in its bordering states, it is essential to determine the emissions from shipping as accurately as possible. Within the Interreg IVb project Clean North Sea Shipping (CNSS) a bottom-up approach was developed and used to thoroughly compile such an emission inventory for 2011 that served as the base year for the current emission situation. The innovative aspect of this approach was to use load dependent functions to calculate emissions from the ships' current activities instead of averaged emission factors for the entire range of the engine loads. These functions were applied to ship activities that were derived from hourly records of Automatic Identification System signals together with a data base containing the engine characteristics of the vessels that traveled the North Sea in 2011. The emission model yielded ship emissions among others of NO_x and SO_2 in high temporal and spatial resolution that were subsequently used in a chemistry transport model in order to simulate the impact of the emissions on pollutant concentration levels. The total emissions of nitrogen reached 540 Gg and of sulfur oxides 123 Gg within the North Sea, which was about twice as much of those of a medium-sized industrialized European state like the Netherlands. The relative contribution of ships to, for example, NO_2 concentration levels ashore close to the sea can reach up to 25 % in summer and 15 % in winter. Some hundred kilometers away from the sea the contribution was about 6 % in summer and 4 % in winter. The relative contribution of the secondary pollutant NO_3^- was found to reach 20 % in summer and 6 % in winter even distant from the shore.

1 Introduction

Land based sources of SO_2 and NO_x have decreased substantially in Europe during the last 20 years, partly because of technical progress in the sectors of traffic, heating and industrial production, and partly because of the political and economic changes in Eastern Europe since 1990. In contrast, measures to control ship emissions were disregarded for a long time. Since a few years, however, the awareness of air pollution by shipping in particular concerning the emission of precursors for particulates has been rising (Eyring et al., 2005a, b; Lauer et al., 2009; Dentener et al., 2006) and political options to decrease ship emissions are discussed. Ship traffic in the North Sea is now recognized by its adjacent states as a relevant source for air pollutants because future projections show that this traffic is likely to grow further during the coming decades. For this reason, the North Sea is accounted for Emission Control Area (ECA) with the objective to reduce the emissions of NO_x and SO_2. Since November 2007 ships have been obliged to use fuel with a sulfur content not higher than 1.5 %. This limit was lowered to 1 % in July 2010 and to 0.1 % as of January 2015. The introduction of a nitrogen control area in the North Sea was planned for 2016. However, this plan is suspended at the moment. In the second greenhouse gas study commissioned by the International Maritime Organisation (IMO) both the increase of ship traffic for the next 40 years and implications of introducing ECAs on emission factors for NO_x and SO_2 are described (Buhaug et al., 2009). Reducing emissions, however, does not necessarily allow to draw conclusions about the actual concentration levels distant from the sources. This is even more true for secondary pollutants like particulate ammonium sulfate or ammonium nitrate that undergo chemical transformations while being transported in the atmosphere. In this study, an emission inventory for ships in the North Sea for 2011 was created with a state-of-the-art modeling approach. The main purpose, however, was to use these emissions with a chemistry transport model (CTM) in order to quantify the effect of sea going ships on air quality (with regard to NO_2, SO_2, ozone and PM) in middle and northern Europe.

Formerly, when little was known about ship activities and the emission behavior of their engines, the only way to estimate emissions of air pollutants from ships was to estimate fuel consumption by means of fuel sales numbers and multiply them with emission factors per units of fuel burned. This method is described in the CORINAIR guidelines (EEA, 2013) and it is partly used to date by the European member states in order to report national emissions to the European Union. It bears, however, large uncertainties because the amount of fuel bunkered in Northern Europe is not necessarily the same amount of fuel consumed there. Deriving emissions from combusted fuel is generally a suitable approach for sulfur dioxide and carbon dioxide emissions that depend only on the mass of fuel and the sulfur or carbon content in that fuel. However, the emissions of substances like NO_x, CO, hydrocarbons and particulate matter (PM) depend strongly on combustion temperature and fuel to air ratio, which are related to the engine load.

With the introduction of the Automatic Identification System (AIS) for ships it became much easier to track ship movements and estimate their actual engine loads provided the necessary engine characteristics are known. When the Clean North Sea Shipping project (CNSS) started, emission factors were only available as constant values that had to be multiplied by the energy or fuel consumption of a ship (Denier van der Gon and Hulskotte, 2010; Matthias et al., 2010). In 2012, Jalkanen et al. (2012) published a study about a ship emission model (STEAM2) that followed an approach similar to the one presented here, also combining AIS signals with a ship characteristics data base. On the one hand, the calculation of the instantaneous engine power is very elaborate in the STEAM2 model, using for example a ship resistance model while the model presented here uses only the ratio between design speed and actual speed. On the other hand, the model presented here uses different emission factor functions for different engine types, vessel sizes and pollutants while Jalkanen et al. (2012) derived load dependency of emission factors from only a few measured engines. Jonson et al. (2014) used results from the STEAM2 emission model for 2011 to estimate the contribution of ships to pollutant concentrations and depositions over Europe. Another study

about the contribution of ships to air pollution that investigated also health effects and external costs was published by Brandt et al. in 2013 (Brandt et al., 2013). It may be valuable to compare the different models and their results in detail, which is, however, beyond the scope of this study. Instead, the plausibility of the ship emissions presented here and their contribution to air pollution was evaluated by performing statistical tests with observed concentrations available from the European Monitoring and Evaluation Programme (EMEP) network (EMEP, 2015).

2 Ship-emissions model

First of all, the bottom-up approach we followed to estimate ship emissions for the year 2011 required activity data about the ships traveling the North Sea. As one of the most effective ways to derive ship activities the evaluation of signals from the automatic identification system (AIS) was established in recent time (Jalkanen et al., 2012). In order to avoid collisions, all ships bigger than 100 gross tons (GT) are obliged to broadcast such a signal every six seconds to indicate – amongst others – their identification number, position, moving status, direction and speed over ground. Some enterprises like IHS Fairplay store these signals for further evaluation and make them available for purchase. On the basis of AIS data it is possible to follow the route of a single ship and to estimate its energy demand, fuel consumption and pollutant exhaust along this route.

The second requirement for a bottom-up inventory are activity based emission factors for different ship types. Such a set of emission factors in the form of load dependent functions resulted from a study of Germanischer Lloyd (GL) (Zeretzke, 2013) within the Inrerreg IVb project Clean North Sea Shipping (CNSS). The model approach developed in this study uses these functions together with interpolation routines, which allows for simulation of ship emissions at nearly arbitrary temporal and spatial resolution. In order to use the ship emissions in a chemistry transport model (CTM) they had to be transferred from latitude-longitude positions to a regularly spaced Eulerian grid.

2.1 Ship routes derived from AIS data

The AIS data base that was acquired from IHS Fairplay contains hourly updated AIS data in the OSPAR region II, defined within The Convention for the Protection of the marine Environment of the North-East Atlantic (the OSPAR Convention) for the whole year 2011 (Fig. 1). According to this data, about 3000 ships with a valid IMO number were active in the North Sea on average per hour in 2011. However, the spatial density of the hourly signals appeared to be too sparse for creating gridded emissions at a resolution required by the used chemistry transport model set up. In addition to this, the coverage of received AIS signals is low in some regions, especially on the open sea. Therefore, the broadcast positions along a ship track were interpolated linearly to complete tracks and to get enough points for transferring the track to the Eulerian grid. At the same time, it was made sure that the interpolated route did not cross solid ground. The vessel whose track was to be reconstructed was identified by its International Maritime Organisation (IMO) or Maritime Mobile Service Identity (MMSI) number contained in the AIS data.

In order to elaborate a temporal emission profile of the ship activities – and hence emissions – the ship emissions for 2011 were calculated as 52 weekly sums (Fig. 2). Using weekly and not daily or hourly data reflects the necessity of having enough points to reconstruct and complete ship tracks. The procedural steps were as follows:

1. Read data sets from the AIS data base of one week.
2. Subset the weekly AIS data by one vessel (IMO or MMSI number).
3. Sort by time stamp: this yields the track of one ship in one week traveling the North Sea.
4. Interpolate the ship track so that it consists of equidistant points. The distance between the track points is set to $\frac{1}{3}$ of the length of a grid cell. Make sure the track does not lead over land.

5. Calculate speed at every track point.

2.2 Handling erroneous records in the AIS data

2.2.1 Implausible ship movements

AIS signals that contained a requested IMO number but did obviously not belong to the current track resulted in an unrealistic movement of the ship. These signals and the therein contained track were detected in case the calculated speed between two track points was 20 % higher than the maximum of all reported speeds in the AIS signals of this track. The second one of these points was then removed from the track and the track was recalculated with the remaining points. If there was more than one implausible point in the track they were removed recursively. The assumption was that the preceding points in the track reflected correct AIS signals. The pitfall is, of course, that the correct points could have been removed and erroneous ones kept.

2.2.2 Mooring ships with unknown demooring point of time

In some cases the AIS signal of a ship disappeared for some time while the ship was mooring and did not reappear immediately after it had demoored. Then, the calculated traveling time between the mooring place M and the next captured AIS position T was too long and the calculated speed was too low (the threshold is 40 % of speed over ground at position T). When this was detected the speed over ground at position T sog(T) was assumed for the whole journey between M and T. In that case, the demooring point of time clock(M) was calculated with the formula below. This approach did not consider that it takes some time until a vessel reaches its cruising speed. The same procedure was applied to correct low speeds in the case where a ship leaves the domain and returns many hours later.

$$\text{clock}(M) = \text{clock}(T) - \frac{\text{distance}[MT]}{\text{sog}(T)}$$

2.3 Attribute ship characteristics to track

Ships in the AIS data base were usually identified by their unique IMO number. In some cases where the IMO number of a record in the data base was missing or invalid vessels were identified by the MMSI number of their broadcasting devices. The corresponding IMO number of that AIS signal was then found as the IMO number that occurred in the data base most frequently together with this MMSI number.

By means of the IMO number of the vessel – whose weekly track was reconstructed as explained above – the technical characteristics needed to calculate the emissions of that track (Table 1) were looked up in a ship characteristics data base that was also acquired from IHS Fairplay or in a second one provided by GL. If the IMO number was present in both data bases and the values were contradictory the values of the IHS data base were used.

All vessels in the data base were divided into seven types (tankers, bulk ships, cargo ships, cruise ships, ferries, tugs and other vessels) and nine size classes defined by gross tonnage (GT) (see Table 1). In several cases single characteristics were missing for a ship. To account for these gaps a look-up table was compiled containing median values per ship class and type whose values were used if not found in the data base. For non-numeric characteristics like fuel type the most frequent one was taken. If no median could be calculated for a particular class the median of a neighboring class was taken.

These medians are used to complete missing data if feasible as follows:

- The GT and type of that ship was found: use class medians for missing characteristics.
- IMO is valid but not found in data bases; AIS contains a valid ship type: use medians of the peak of the frequency distribution for this ship type (Fig. 3).

2.4 Emission calculation

Energy consumption, fuel consumption and the emissions of NO_x, SO_2, CO, NMVOC, CO_2, mineral ash, sulfuric acid, black carbon (BC) and primary organic carbon (POA) were calculated for every track point where the calculated speed was larger than 2 kn. 2 kn was assumed to be the threshold indicating that the ship was neither mooring nor maneuvering. This means, of course, that the emissions of ships in ports are underestimated. Because ports cover only a small part of the entire area of the applied regional model, we considered this lack to be acceptable as a first approach. In future versions the inclusion of a port emissions model is planned. Consumption and emissions depend on the actual load L of the ship which was calculated with the speed at MCR and the calculated actual speed scalc. Calculating the energy consumption E was then straightforward using MCR, the actual load and the time difference between two track points Δt.

$$L = \left(\frac{\text{speed}_{\text{MCR}}}{\text{scalc}}\right)^3$$

$$E = L \times \text{MCR} \times \Delta t$$

For auxiliary engines the load for moving ships was kept constant at 0.3. Fuel consumption and pollutant emissions Em were calculated by multiplying the energy consumption E with specific emission factors EF (in g kWh^{-1}), which were developed by Zeretzke from GL. These emission factors are a function of load L, propulsion type P (diesel electric or direct/gear drive), fuel type F (Heavy Fuel Oil or Marine Diesel Oil) and year of build Y.

$$\text{EF} = f(L, P, F, Y)$$

$$\text{Em} = \text{EF} \times E$$

The load was kept between 1 and 0.25 because the emission factors are only applicable for this range according to Zeretzke. If the maximum speed of the ship

($\text{speed}_{\text{MCR}}$) that was stored in the ship characteristics data base was lower than the maximum reported speed (sog) along the track – corrected for implausible track points – $\text{speed}_{\text{MCR}}$ was set to max(sog). Loads lower than 0.25 were simply set to 0.25. An exception was the calculation of BC emissions because it is known that these increase significantly at low loads. We used the formulas below to calculate a correction factor for BC emissions f_{BC}. This piece-wise linear fit to an average relation between engine load and BC emissions was derived from a diagram in Lack and Corbett (2012).

$$f_{\text{BC}} = \frac{6 - 0.12 \times L}{1.2} \qquad 0 < L \leq 0.25$$

$$f_{\text{BC}} = \frac{3 - 0.052 \times (L - 0.25)}{1.2} \qquad 0.26 < L \leq 0.50$$

$$f_{\text{BC}} = \frac{1.7 - 0.02 \times (L - 0.50)}{1.2} \qquad 0.51 < L \leq 0.75$$

$$f_{\text{BC}} = \frac{1.2 - 0.008 \times (L - 0.75)}{1.2} \qquad 0.76 < L \leq 1$$

2.5 Transferring the line sources to the model grid

The last step was to transfer these line source emissions to the grid cells of the model domain. The model domain consists of equally spaced grid cells in a Lambert conformal projection. Therefore, the track points defined by latitude-longitude coordinates were converted to Lambert x–y coordinates. Next, the grid cells in which the track points lie were found and all emissions in a cell summed up and added to the domain.

2.6 SO_2 emissions outside the ECA zone

Most of the AIS records lie within the ECA zone where 1 % S in ship fuels is allowed whereas outside the ECA areas the threshold is 3.5 % S. In fact, the average sulfur content of the heavy fuel oil (HFO) used in international shipping is 2.7 %. Most of the ships traveling the areas outside and inside ECAs have the technical possibility to

change fuels. Thus, for simplicity it was assumed that outside the ECA high sulfur and inside the ECA low sulfur fuel was used in general. Therefore, sulfur emissions were calculated for 1 % S in the whole domain and then a factor of 2.7 was applied to grid cells outside the ECA.

3 Ship emission inventory

Most of all, the exhaust of pollutants is connected with the fuel consumption and, thus, with the energy demand of the ships. Therefore, the sections of the North Sea where the highest emissions of pollutants occurred were those where the majority of the big ships with high energy demand travel. These are the English Channel and the route along the North Sea coast between Belgium and Germany because the largest ships head for the three biggest ports in Europe, Rotterdam, Antwerp and Hamburg. From there, goods are distributed to smaller ports with medium-sized ships that account for regional and inner-European shipping. The main routes for medium-sized ships extend between central-western Europe and Scandinavia. It is a fundamental plausibility check for the bottom-up emission approach that these main shipping lanes could be reconstructed from the AIS data base (Fig. 4). Thus, the emissions of smaller ships were spread all over the North Sea while the large vessels that only travel certain routes along the coasts were responsible for the peak values there.

Table 2 shows the share of ships of different sizes on the total fuel consumption as well as of NO_x and SO_2 emissions on the North Sea. It quantifies also the differences if emissions of an average ship of a size class were compared or if the pollutant exhaust was related to the amount of freight transported per size class. It is evident that the share of air pollution of the large ships was big if single ships were compared but small if it was related to the freight volume of the ships. This suggests that using large vessels to transport large amount of goods causes less emissions than using smaller vessels for the same amount of goods, provided, of course, that the large vessels use their full freight capacity. In this comparison, however, it should be kept in mind that the amount

of goods distributed by medium sized ships to smaller ports in the North and Baltic Sea depends on the freight shipped with large vessels from all over the world. The total calculated ship emissions in 2011 in the study area were less than those of the big industrial countries like Germany, UK and France, but more than those of smaller countries (Fig. 5).

A closer look at Table 2 reveals that the relations are not exactly the same for all pollutants. The exhaust of sulfuric acid and SO_2 depends both on the fuel consumption and on the sulfur contents of the fuels used. On the one hand, the specific fuel consumption in $g\,kWh^{-1}$ of smaller ships is higher than that of bigger ones. On the other hand, 95 % of the large ships use high sulfur fuel in contrast to 75 % of the medium-sized ships, so that it could be expected that the share of sulfur emissions for larger ships was higher even if the share in fuel consumption was lower. This relation should be reversed for NO_x exhaust because the combustion temperature in smaller engines is higher which promotes the creation of oxidized nitrogen (Zeretzke, 2013). In our data set of 2011, this effect appeared to be only weakly pronounced. Ships larger than 60 000 GT consumed 83.1 % of the fuel while causing 83.6 % of SO_2 and 82.7 % of the NO_x emissions, whereas smaller ships consumed 16.9 % of the fuel and caused 16.4 % of the SO_2 and 17.3 % of the NO_x emissions (Table 2).

The total ship emissions in 2011 for the model area amounted to 540 Gg for NO_x and 123 Gg for SO_2. At the same time, the officially reported emissions for the North Sea were 798 Gg for NO_x and 192 Gg for SO_2 (EMEP/CEIP, 2014). Even if the areas are not the same the differences seem to be remarkable. However, recent investigations by Vinken et al. (2014) also suggested that the officially reported ship emissions might be overestimated by about 35 %. A further discussion of these differences would require to investigate the differences of the methods applied to create the inventories, which is not intended in this paper.

4 Model set up for the chemistry-transport simulations

The contribution of shipping to air quality in the North Sea area can be determined by combining accurate emission inventories with advanced three-dimensional chemistry transport (CTM) models. A CTM imports emissions and uses meteorological data like wind speed, wind direction, radiation and temperature to simulate transport and chemical transformation of pollutants in the atmosphere. In this way, the CTM developed by the US Environmental Protection Agency, called Community Multi-scale Air Quality (CMAQ) model, was used to calculate air concentrations of a number of pollutants depending on the input emissions. The CMAQ model was used in its version 4.7.1 with the CB05 chemistry mechanism (Byun and Ching, 1999; Byun and Schere, 2006). It was run for an entire year with a spin up time of 2 weeks and a data output time step of one hour. Boundary conditions for the model were from the TM5 global chemistry transport model system (Huijnen et al., 2010). The meteorological fields that drive the chemistry transport model were produced with the COSMO-CLM mesoscale meteorological model for the year 2008 (Rockel et al., 2008). This year was chosen because it did not include very unusual meteorological conditions in central Europe and can therefore be considered to represent average weather conditions in Europe. The simulation of atmospheric chemical processes is of particular importance for estimating concentrations of secondary pollutants which are not emitted directly but formed from emitted gases by chemical reaction. The most prominent one is ozone, whose formation is influenced by NO_x. Also very important for health and environment is secondary particulate matter that emerges from gaseous emissions, mostly NO_x and SO_2, and constitutes the largest portion of the noxious fine particulate matter. Emissions from other sources like traffic, industry, households and agriculture were taken from official European emission inventories and made model ready with the Sparse Matrix Operator Kernel Emissions model for Europe (SMOKE-EU Bieser et al., 2011). Model runs were performed both using all available emissions including the ship emission inventory and

using land based emissions exclusively. The resulting concentration differences between these runs revealed the impact of shipping emissions.

5 Simulation results

5.1 Validation of simulations through comparison to observations

Several air pollutants are routinely measured by European authorities. They are available for download via the EMEP internet sites (EMEP, 2015) and can be used to validate model results. Even if it must be taken into account that the location where the measurement takes place may not be fully representative for the model grid cell this location belongs to and the overall measurement uncertainty of the observations is not known this comparison provides a good indication for the plausibility of the simulated concentrations. The comparison involves both a graphical comparison of concentration time series and the calculation of some statistical parameters. The authors decided to use only those stations for model evaluation at which values were provided on more than 200 days.

The agreement between measurements and simulations is different at different measurement stations. Very low background concentrations are usually both difficult to measure and to predict correctly with models. For assessing the agreement between observations and simulations the correlation coefficient and the normalized mean bias (NMB) were used (Tables 3 through 5). With only a few exceptions both the measured and modeled concentrations were found to be not normal but logarithmically distributed. In these cases, the mean values shown are geometric means and the correlation was calculated as Spearman rank correlation. Only the NMB was calculated from original concentration values because the authors regarded it as a non-parametric estimator.

Without knowing the measurement conditions and the observation site it is hardly possible to explain the differences exactly. Nonetheless, some cautious but plausible conclusions can be drawn.

5.1.1 Assessment of the base case model results

Because observations of NO_2 are usually available as daily averages, the hourly model output was also recalculated to daily mean values. The resulting time series were compared to the daily mean of observations at measurement stations in North Sea bordering states (Fig. 6). As often seen with air quality models, CMAQ tended to predict lower NO_2 concentrations than measurements would suggest (Bessagnet et al., 2014), which can be seen by the negative NMB. If the time profile of the predicted values resembles that of the observations and if peak values in the measurements are met by the predictions a correlation should be found. Without testing the significance of the correlation explicitly we consider a correlation coefficient of more than 0.5 to indicate a correlation whereas we speak of a good correlation at values of 0.7 and above. Concerning NO_2, 17 out of 29 stations had a correlation coefficient of at least 0.7, whereas only three showed a coefficient below 0.5 (Table 3). Stations with low correlation are those that lie in a difficult heterogeneous terrain like rocky coastal areas or on a small island in the sea or where the background concentrations are very low with no peaks but only random variations of the signal.

SO_2 concentrations are generally lower than NO_2 concentrations. This may be a reason for the correlation coefficients being lower than for NO_2. None of the 15 available stations showed a correlation coefficient higher than 0.7 (Table 4). At least, seven of them had a value of more than 0.5. Another reason for low correlations could be that SO_2 shows nearly no seasonality. In contrast to this, O_3 expresses the most significant seasonality of all investigated substances. As the model succeeded in modeling this seasonal concentration differences, only three out of 36 stations seemed to show no correlation at all. On the other hand, only seven stations showed a good correlation, which reflects the difficulties in modeling the short term variability of ozone (Table 5).

Similar to ozone, nitrate (NO_3^-) and sulfate (SO_4^{2-}) which constitute the major part of inorganic particulate matter are not directly emitted from the engines, but rather formed in the air by chemical reactions of NO_2 and SO_2. As the formation of these particulates is a complicated and not yet fully understood process the model results are presumably less reliable than for gaseous compounds. Also, the sampling and measurement process is fairly complicated. The agreement between model and observations seemed to be better for nitrate than for sulfate. On the other hand, much less stations were available to evaluate the nitrate simulations (Tables 6 and 7). Six out of nine stations with nitrate measurements presented a correlation coefficient higher than 0.7 while none of the 24 stations for sulfate did. The reason for this is probably the weak seasonality of sulfate in contrast to nitrate. The concentrations of particulate nitrate are notably dependent on ammonia concentrations in the atmosphere, and these are higher in summer than in winter. In contrast, particulate sulfate is nearly invariant to the concentration variations of ammonia.

5.1.2 Differences between the base case and the no-ship-emissions case

It is evident that at coastal stations where ship emissions increase the background concentrations of the pollutants the model bias of the under-predicted substances like NO_2 decreases. This can be shown exemplary for the Danish island Anholt (Fig. 7) where the NMB changed from to −0.69 to −0.37 (Table 3). Some peaks that had been missed by the simulations without ship emissions were met. For this reason, not only the bias decreased but also the correlation increased at some stations if ship emissions were included. The significance of the increase of correlation between simulations and observations was tested by calculating the Fisher z transformation of the two correlation coefficients for the different model runs and testing the alternative hypothesis “greater than” at a significance level of 0.9. This means, it was accepted that the correlation at a certain station increased by including ship emissions if the probability of this assumption was larger than 90 %. The significance of the difference of model biases was

validated by performing a one-sided *t* test between the model results with and without including ship emissions. As mentioned above, values were logarhythmized if necessary. It can be stated that those stations where bias and correlation were enhanced significantly are most likely to be influenced by ship emissions.

Concerning NO_2 significant correlation increases could be stated for Zingst, Keldsnor, Anholt, Yarner Wood, Lullington Heath, St. Osyth and Raö – the latter also lying on an island like Anholt. In the densely populated Netherlands and Belgium where concentrations are generally higher than in other coastal regions around the North Sea the relative contribution of ships was quite small. Actually, no significant concentration increase could be found for the Belgian stations, and in the Netherlands an increase could only be found for stations close to the sea. For the rest of the studied area all stations close to the sea showed concentration increases and even Neu Globsow in the German hinterland.

Only four stations in the Baltic Sea (the most eastern part of the Baltic Sea was also in the model domain) showed significantly increased correlations concerning SO_2. However, stations that showed increased NO_2 concentrations also showed increased SO_2 concentrations which underlines the influence of ships for these sites. When looking at O_3 one would expect that the correlations only were increased at those stations where also NO_2 had a better correlation. There were, however, three stations, Westerland, Zingst and Ulborg where increased correlations for ozone could be verified, but not for NO_2. This can neither be unambiguously explained by ship emissions nor by the model chemistry. On the one hand, O_3 lives longer than NO_2, which could be the reason that the ship influence is easier to detect with O_3. On the other hand, the tree mentioned measurement stations lie close to the shipping lanes and the atmospheric life-time of the substances might not play such a big role. Therefore, the ambiguities could also be an issue of the measurement data. There were in total 8 stations with increased ozone correlations, all of them placed close to the sea.

It was already mentioned that it is both difficult to model and to measure particulate NO_3^-, and therefore it is no surprise that no significant increase of correlation coeffi-

cients between the two model runs could be confirmed. The same can be said about particulate sulfate with one exception at Keldsnor. All stations where the modeled NO_2 concentrations increase significantly also presented significantly increased nitrate concentrations. The same relation would be expected between SO_2 and sulfate. It could, however be not confirmed for the stations Waldhof, Birkenes and Vredepeel. In this regard, it should be mentioned that results of statistical testing only allow to state that the effect could not be verified. They are always dependent on the underlying data and do not necessarily reflect reality. Still, it can be generalized that the concentration levels for particulates increased at stations close to the shipping lanes.

5.2 Concentration patterns over Northwest Europe

The highest pollutant concentrations typically occurred over land at highly populated or industrialized areas. Some of these areas in France, Belgium, Holland and UK lie relatively close to the shore and therefore experienced moderate concentration increases by ship emissions. While sites east of the English Channel showed increases of about 10 % much less increase could be discovered along the eastern coast of the UK (see for example NO_2, Fig. 8). The reason is that pollutant clouds from the shipping lanes passing the Channel are transported towards the continent by the prevailing westerly and south-westerly wind directions. In less populated areas such as Scotland and large parts of Scandinavia pollution levels were generally lower than in the regions mentioned above. This is why the relative pollution increase by ships was up to 50 % in summer and between 10 and 20 % in winter. Apart from the presence of other sources, the relative influence of ship exhaust on air pollutant concentrations also depends on the reaction rates of primary pollutants to form secondary pollutants. These are higher at higher temperatures, which would increase concentrations of secondary pollutants in summer and decrease them in winter. On the other hand, the coagulation of particulates is retarded at lower temperatures, which would suggest lower concentrations of particle bound secondary pollutants like NO_3^- and SO_4^{2-} in summer. Northern Germany and Denmark can be considered as coastal regions and are surrounded by numerous

shipping lanes. There, the contribution of shipping emissions to NO_2 is around 15 % in winter and 25 % in summer. Similarly, the contributions concerning SO_2 are about 12 % in winter and 30 % in summer (Fig. 9). Some hundred kilometers away from the sea in the German hinterland the contributions to SO_2 are 5 % in summer and 2 % in winter while for the secondary particulate sulfate the contributions are 8 % in summer and 3 % in winter (Fig. 10).

Along the major shipping lanes between UK and Germany the pollution levels were comparable to those of mildly polluted land sites in Europe. However, the concentration maps (Figs. 8 through 14) indicated that nowhere in the investigated domain the contribution of ship emissions to any pollutant was 100 %. This means that emissions produced ashore and substances that enter the domain through the boundaries were transported over the North Sea. Where these influences were low the contribution of ship emissions were the highest provided ships operated in these regions. The most significant example for this was the western entrance to the English Channel where the ship emissions were responsible for over 90 % of NO_2 and SO_2 concentrations.

5.2.1 NO_2 and SO_2

While for NO_2 and SO_2 the overall concentrations were higher in the colder months Figs. 8 and 9 suggest that the absolute contribution of ships is lower in these months. One of the largest sources of land based pollution is heating, which is subject to seasonality. Therefore, the relative contribution of ship engines to pollution levels is lower in winter than in summer because, while the shipping activity is nearly the same all over the year, more pollution from land based sources is produced in winter than in summer. Due to the relatively high emissions of land based sources in winter only slight concentration changes over land in a small slice at the land-sea border were noticeable. In summer, this slice was a little broader indicating that the shipping influence could be recognized further inland than in winter. SO_2 concentrations were a little lower than NO_2 concentrations. The relative contribution of ships within the North Sea was also a little lower with the general spatial pattern being similar. However, the influence of

ships was high at the domain borders because the ships are allowed to use there fuel with higher sulfur content.

5.2.2 $PM_{2.5}$

The maps of simulated $PM_{2.5}$ concentrations suggested in some regions a large relative contribution from ships in the summer months even far inland. This emphasized that the influence of ship emissions on particulate matter in general could be seen further away from the shipping lanes than it is the case for NO_2 and SO_2, the most important precursors of these secondary pollutants. The influence of ship emissions was further emphasized by the fact that concentration peaks in the time-series (Fig. 12) were accompanied by relatively large reductions if ship emissions had been omitted. The main constituents of $PM_{2.5}$ are ammonium sulfate and ammonium nitrate, whereas nitrate and sulfate originate from oxidation of NO_2 and SO_2. While these reactions are taking place the pollutant clouds can be transported inland (Fig. 13). These reaction rates depend, however, on temperature, solar radiation and the availability of reaction partners like OH and NH_3, which means that the reaction conditions are much better in summer than in winter.

5.2.3 Ozone

The formation of ozone is, most of all, driven by solar radiation and temperature. Thus, there is a clear summer to winter gradient. It is also evident that the contribution of ships can selectively be very significant, both in terms of increasing the O_3 levels noticeably and decreasing them. The latter is the case in the Channel where massive emissions of NO_x in the absence of VOCs result in degradation of ozone. Figure 14 illustrates that ozone concentrations were increased by more than 10 % along the Scandinavian coasts where no other relevant NO_x sources but enough VOC was present to form additional ozone.

For the purpose of assessing air quality, ozone concentrations are usually denoted as eight-hour maximum concentrations. This is the maximum of eight-hour means calculated as gliding average for one day. A value of 120 µg m^{-3} was recommended by WHO in 2000 as the value below which health risks are low. The same value has been defined as a target value in the EU recommending that it should not be exceeded on more than 25 days per year within three subsequent years. An analysis of the daily 8 h maximum ozone values in selected coastal regions around the North Sea (Fig. 1) revealed that in Germany, the Netherlands and Belgium and in the UK a concentration of 120 µg m^{-3} was exceeded on more than 25 days (Table 8). Excluding shipping emissions reduced this number significantly in the UK and in Germany. In the Netherlands and Belgium the effects were much smaller because of the high NO_x emissions from other sources.

6 Summary and conclusions

A multi-model approach to evaluate the impact of shipping on air quality was developed and applied to the North Sea and its bordering states for the year 2011. This approach involved developing a bottom-up emissions model for sea going ships and integrating this into a well established modeling system (CCLM, SMOKE-EU and CMAQ) to simulate atmospheric transport and chemical transformations of the emitted pollutants.

It is evident that the predictive ability of the modeling system for compounds that tend to be underestimated by the model improves by including ship emissions – particularly in coastal regions. An evaluation of the correlation and the bias between measured and modeled concentrations suggested that the agreement between model and observations improved generally at coastal stations. The less polluted a measurement site is by land-based sources like traffic or industry, the more enhancement of the prediction could be observed. This underlines both the necessity to include a proper representation of shipping emissions into emission inventories for air quality modeling and the plausibility of the model presented here.

The greatest benefit of a sophisticated bottom-up approach like the one presented here is the possibility to use it for creating and evaluating different emission scenarios (Matthias et al., 2015).

Running the chemistry transport model CMAQ with and without including ships in the emission inventory revealed that high relative contributions to primary gaseous pollutants concentrated at hot spots along the main shipping lanes. At the same time, the relative contribution to secondary pollutants like particulates and ozone was lower but distributed over a larger area. Even if the contribution of ships to concentration levels of air pollutants in densely populated areas is low it is possible that ship emissions rise the background concentrations sufficiently high that threshold values are more likely to be exceeded and air pollution standards missed.

Acknowledgements. This work was partly funded by the European Regional Development Fund (ERDF) within the Interreg IVB projects Clean North Sea Shipping (CNSS) and CNSS Improved Dissemination and Impact (CNSS-IDI). US EPA is gratefully acknowledged for the use of CMAQ, we thank Twan van Noije (KNMI) for providing TM5 model data.

The article processing charges for this open-access publication were covered by a Research Centre of the Helmholtz Association.

References

Bessagnet, B., Colette, A., Meleux, F., Rouil, L., Favez, O., Cuvelier, C., Thunis, P., Tsyro, S., Stern, R., Manders, A., Kranenburg, R., Aulinger, A., Bieser, J., Mircea, M., Briganti, G., Cappelletti, A., Calori, G., Finardi, S., Silibello, C., Ciarelli, G., Aksoyoglu, S., Prévot, A., Pay, M.-T., Baldasano, J., Garcia Vivanco, M., Garrido, J. L., Palomino, I., Martín, F., Pirovano, G., Roberts, P., Gonzalez, L., White, L., Menut, L., Dupont, J.-C., Carnevale, C., and Pederzoli, A.: The EURODELTA III exercise – model evaluation with observations issued from the 2009 EMEP intensive period and standard measurements in Feb/Mar 2009, Tech. Rep. 1/2014, Cooperative programme for monitoring and evaluation of the long-range transmission of air pollutants in Europe – EMEP, 2014. 11291

Bieser, J., Aulinger, A., Matthias, V., Quante, M., and Builtjes, P.: SMOKE for Europe – adaptation, modification and evaluation of a comprehensive emission model for Europe, Geosci. Model Dev., 4, 47–68, doi:10.5194/gmd-4-47-2011, 2011. 11289

Brandt, J., Silver, J. D., Christensen, J. H., Andersen, M. S., Bønløkke, J. H., Sigsgaard, T., Geels, C., Gross, A., Hansen, A. B., Hansen, K. M., Hedegaard, G. B., Kaas, E., and Frohn, L. M.: Assessment of past, present and future health-cost externalities of air pollution in Europe and the contribution from international ship traffic using the EVA model system, Atmos. Chem. Phys., 13, 7747–7764, doi:10.5194/acp-13-7747-2013, 2013. 11281

Buhaug, Ø, Corbett, J., Endresen, Ø, Eyring, V., Faber, J., Hanayama, S., Lee, D., Lee, D., Lindstad, H., Markowska, A., Mjelde, A., Nelissen, D., Nilsen, J., Pålsson, C., Winebrake, J., Wu, W., and Yoshida, K.: Second IMO GHG Study, Tech. rep., International Maritime Organization (IMO), London, UK, 2009. 11279

Byun, D. and Ching, J.: Science Algorithms of the EPA Models-3 Community Multiscale Air Quality Modeling System, Epa/600/r-99/030, US Environmental Protection Agency, Office of Research and Development, Washington DC, 1999. 11289

Byun, D. and Schere, K.: Review of the governing equations, computational algorithms, and other components of the models-3 community multiscale air quality (CMAQ) modeling system, Appl. Mech. Rev., 59, 51–77, 2006. 11289

Denier van der Gon, H. and Hulskotte, J.: Methodologies for estimating shipping emissions in the Netherlands, BOP reports 500099012, this is a publication of the Netherlands Research Program on Particulate Matter, Netherlands Environmental Assessment Agency, (PBL), Bilthoven, the Netherlands, 2010. 11280

Dentener, F., Kinne, S., Bond, T., Boucher, O., Cofala, J., Generoso, S., Ginoux, P., Gong, S., Hoelzemann, J. J., Ito, A., Marelli, L., Penner, J. E., Putaud, J.-P., Textor, C., Schulz, M., van der Werf, G. R., and Wilson, J.: Emissions of primary aerosol and precursor gases in the years 2000 and 1750 prescribed data-sets for AeroCom, Atmos. Chem. Phys., 6, 4321–4344, doi:10.5194/acp-6-4321-2006, 2006. 11279

EEA: EMEP/EEA air pollutant emission inventory guidebook 2013, Tech. Rep. 12, European Environment Agency, doi:10.2800/92722, 2013. 11280

EMEP: The European Monitoring and Evaluation Programme, available at: http://www.emep.int/, last access: January 2015. 11281, 11290

EMEP/CEIP: Present state of emission data, available at: http://www.ceip.at/webdab_emepdatabase/reported_emissiondata, last access: June 2014. 11288

Eyring, V., Kohler, H. W., Lauer, A., and Lemper, B.: Emissions from international shipping: 2. Impact of future technologies on scenarios until 2050, J. Geophys. Res.-Atmos., 110, D17306, doi:10.1029/2004JD005619, 2005a. 11279

Eyring, V., Kohler, H. W., van Aardenne, J., and Lauer, A.: Emissions from international shipping: 1. The last 50 years, J. Geophys. Res.-Atmos., 110, D17305, doi:10.1029/2004JD005620, 2005b. 11279

Huijnen, V., Williams, J., van Weele, M., van Noije, T., Krol, M., Dentener, F., Segers, A., Houweling, S., Peters, W., de Laat, J., Boersma, F., Bergamaschi, P., van Velthoven, P., Le Sager, P., Eskes, H., Alkemade, F., Scheele, R., Nédélec, P., and Pätz, H.-W.: The global chemistry transport model TM5: description and evaluation of the tropospheric chemistry version 3.0, Geosci. Model Dev., 3, 445–473, doi:10.5194/gmd-3-445-2010, 2010. 11289

Jalkanen, J.-P., Johansson, L., Kukkonen, J., Brink, A., Kalli, J., and Stipa, T.: Extension of an assessment model of ship traffic exhaust emissions for particulate matter and carbon monoxide, Atmos. Chem. Phys., 12, 2641–2659, doi:10.5194/acp-12-2641-2012, 2012. 11280, 11281

Jonson, J. E., Gauss, M., Jalkanen, J. P., Nyíri, A., and Johansson, L.: EMEP Model Calculations of the Effects of Ship Emissions in the Baltic Sea and the North Sea, Clean Shipping Currents, 2014. 11280

Lack, D. A. and Corbett, J. J.: Black carbon from ships: a review of the effects of ship speed, fuel quality and exhaust gas scrubbing, Atmos. Chem. Phys., 12, 3985–4000, doi:10.5194/acp-12-3985-2012, 2012. 11286

Lauer, A., Eyring, V., Corbett, J. J., Wang, C. F., and Winebrake, J. J.: Assessment of near-future policy instruments for oceangoing shipping: impact on atmospheric aerosol burdens and the earth's radiation budget, Environ. Sci. Technol., 43, 5592–5598, 2009. 11279

Matthias, V., Bewersdorff, I., Aulinger, A., and Quante, M.: The contribution of ship emissions to air pollution in the North Sea regions, Environ. Pollut., 158, 2241–2250, doi:10.1016/j.envpol.2010.02.013, 2010. 11280

Matthias, V., Aulinger, A., Backes, A., Bieser, J., Geyer, B., Quante, M., and Zeretzke, M.: The impact of shipping emissions on air pollution in the Greater North Sea region – Part 2: Scenarios for 2030, Atmos. Chem. Phys. Discuss., 15, 11325–11368, doi:10.5194/acpd-15-11325-2015, 2015. 11298

Rockel, B., Will, A., and Hense, A.: The Regional Climate Model COSMO-CLM(CCLM), Meteorol. Z., 17, 347–348, 2008. 11289

Vinken, G. C. M., Boersma, K. F., van Donkelaar, A., and Zhang, L.: Constraints on ship NO_x emissions in Europe using GEOS-Chem and OMI satellite NO_2 observations, Atmos. Chem. Phys., 14, 1353–1369, doi:10.5194/acp-14-1353-2014, 2014. 11288

Zeretzke, M.: Entwicklung eines Modells zur Quantifizierung von Luftschadstoffen, die durch Schiffsdieselmotoren auf See emittiert werden, Master's thesis, Technische Universität Hamburg-Harburg, 2013. 11281, 11288

Table 1. Class medians of characteristics for cargo ships. MCR is the maximum continuous rating in kWh, speed the design speed in kn, RPM the revolutions per minute, *Y* the year of build and power aux. the installed power of auxiliary engines in kWh.

class	GT	MCR	speed	RPM	*Y*	power aux
1	< 100	–	–	–	–	–
2	< 1600	–	–	–	–	–
3	< 3000	749	11.5	750	1995	328
4	< 5000	2400	12.5	600	1997	550
5	< 10 000	4690	15.5	500	2004	1213
6	< 30 000	10 400	19	127	2002	2284
7	< 60 000	21 068	22	104	2005	7400
8	< 100 000	57 100	25	102	2005	9416
9	> 100 000	68 640	24.9	104	2010	13 188

Table 2. Percentile share of different ship sizes in fuel consumption and emissions within the model domain in 2011; middle: normalized by the number of ships in every class; right: normalized by the transported freight volume in every class (estimated from the gross tonnage).

					normalized by counts			normalized by freight		
class	GT	fuel	SO_2	NO_x	fuel	SO_2	NO_x	fuel	SO_2	NO_x
2	< 1600	1.6	1.6	1.4	0.9	0.9	0.8	34.1	33.9	31.9
3	< 3000	1.7	1.7	1.6	0.6	0.6	0.5	5.6	5.6	4.9
4	< 5000	16.8	16.8	17.6	2.6	2.6	2.7	14.9	14.7	16.2
5	< 10 000	7.9	7.9	7.8	3.7	3.8	3.6	12.1	12.3	12.3
6	< 30 000	25.1	25.4	24.5	9.1	9.4	8.8	10.4	10.7	10.6
7	< 60 000	18.7	18.8	18.7	14.9	15.2	14.8	8.4	8.5	8.8
8	< 100 000	21.3	21	21.1	28.6	28.6	28	8.2	8.1	8.4
9	> 100 000	7	6.8	7.3	39.6	39	40.8	6.4	6.2	6.9

Table 3. Comparison of simulated NO_2 concentrations with observations in $\mu g\,m^{-3}$. Values that are significantly different between the base case and the no-ships case are printed in bold.

	base case			no ships			observations	
station	corr	NMB	mean	corr	NMB	mean	mean	# samples
Offagne	0.7	−0.33	1.3	0.71	−0.36	1.25	2.1	332
Eupen	0.62	0	3.08	0.6	−0.04	2.9	3.27	344
Vezin	0.72	−0.25	2.86	0.72	−0.27	2.75	4.28	346
Westerland	0.77	−0.62	**0.55**	0.76	−0.76	0.29	1.44	349
Waldhof	0.83	−0.43	1.13	0.82	−0.47	1.05	2.37	350
Neuglobsow	0.74	−0.28	**0.96**	0.76	−0.33	0.87	1.51	359
Schmücke	0.71	−0.16	1.38	0.71	−0.18	1.35	1.79	355
Zingst	**0.72**	−0.38	**1.1**	0.61	−0.61	0.54	1.95	359
Keldsnor	**0.71**	−0.39	**1.2**	0.57	−0.67	0.49	2.04	344
Anholt	**0.65**	−0.45	**0.72**	0.45	−0.73	0.3	1.38	322
Eskdalemuir	0.45	−0.41	0.62	0.44	−0.45	0.57	1.41	364
Yarner Wood	**0.54**	−0.42	**0.82**	0.45	−0.54	0.62	1.57	245
High Muffles	0.72	−0.09	**1.27**	0.71	−0.14	1.14	1.57	287
Aston Hill	0.64	−0.21	0.97	0.64	−0.26	0.89	1.6	295
Bush	0.67	−0.54	0.87	0.67	−0.56	0.81	2.24	258
Harwell	0.7	−0.01	2.56	0.68	−0.05	2.42	2.52	310
Ladybower Res.	0.66	0.11	2.08	0.66	0.07	2.01	2.16	251
Lullington Heath	**0.65**	−0.31	**1.54**	0.53	−0.46	1.05	2.52	360
Narberth	0.56	−0.66	**0.31**	0.55	−0.75	0.18	1.42	350
Wicken Fen	0.73	−0.07	2.25	0.73	−0.12	2.11	2.64	355
St. Osyth	**0.74**	−0.34	**2.06**	0.61	−0.47	1.54	3.18	324
Market Harborough	0.82	−0.14	2	0.82	−0.18	1.9	2.67	365
Eibergen	0.8	−0.36	2.39	0.81	−0.39	2.23	4.64	361
Vredepeel	0.79	−0.45	3.06	0.78	−0.47	2.89	6.49	365
Cabauw	0.74	−0.32	**3.33**	0.77	−0.39	2.89	5.62	364
De Zilk	0.77	−0.44	**2.03**	0.78	−0.55	1.38	4.18	337
Birkenes	0.39	0.76	**0.5**	0.33	0.53	0.43	0.26	361
Hurdal	0.46	3.04	2.1	0.44	2.98	2.05	0.45	360
Råö	**0.6**	−0.5	**0.53**	0.53	−0.73	0.27	1.12	364

Table 4. Comparison of simulated SO_2 concentrations with observations in $\mu g\,m^{-3}$. Values that are significantly different between the base case and the no-ships case are printed in bold.

	base case			no ships			observations	
station	corr	NMB	mean	corr	NMB	mean	mean	# samples
Westerland	0.45	0.17	**0.21**	0.44	−0.15	0.08	0.32	242
Waldhof	0.53	0.85	0.47	0.53	0.76	0.41	0.31	237
Neuglobsow	0.58	0.48	**0.34**	0.61	0.37	0.27	0.29	240
Schmücke	0.65	0.4	0.58	0.66	0.37	0.55	0.49	311
Zingst	**0.43**	0.45	**0.46**	0.26	−0.09	0.15	0.37	236
Tange	0.63	0.61	**0.14**	0.59	0.3	0.1	0.12	350
Keldsnor	**0.68**	0.53	**0.49**	0.54	−0.06	0.19	0.35	339
Anholt	**0.62**	0.11	**0.21**	0.44	−0.31	0.09	0.22	339
Ulborg	0.52	0.4	**0.12**	0.47	0.1	0.07	0.12	340
Narberth	0.07	−0.78	**0.22**	0.05	−0.85	0.1	1.64	245
Wicken Fen	0.33	−0.2	1.34	0.33	−0.23	1.29	2.11	363
Bilthoven	0.32	0.43	1.27	0.31	0.34	1.16	1.03	224
Vredepeel	0.49	1.38	1.25	0.48	1.32	1.19	0.65	251
De Zilk	0.45	0.45	**1.27**	0.42	0.32	1.04	1.2	254
Råö	**0.38**	−0.25	**0.15**	0.23	−0.5	0.07	0.26	346

Table 5. Comparison of simulated O_3 concentrations with observations in $\mu g\,m^{-3}$. Values that are significantly different between the base case and the no-ships case are printed in bold.

	base case			no ships			observations	
station	corr	NMB	mean	corr	NMB	mean	mean	# samples
Westerland	**0.66**	0.09	72.15	0.58	0.06	70.63	63.42	365
Waldhof	0.75	0.28	64.57	0.74	0.26	63.88	45.73	365
Neuglobsow	0.68	0.25	68.27	0.65	0.23	66.82	54.45	365
Schmücke	0.69	0.04	67.81	0.69	0.03	67.25	64.21	365
Zingst	**0.68**	0.29	70.37	0.62	0.26	68.94	54.62	365
Keldsnor	**0.69**	0.22	71.34	0.62	0.19	69.62	58.29	365
Ulborg	**0.7**	0.09	**72.23**	0.64	0.06	70.12	66.16	332
Lille Valby	0.69	0.24	67.81	0.64	0.21	66.18	54.89	365
Eskdalemuir	0.62	0.21	67.38	0.64	0.18	66.28	54.31	346
Yarner Wood	0.53	0.22	74.37	0.54	0.2	73.26	60.84	344
High Muffles	0.64	0.17	66.72	0.65	0.14	65.39	55.17	313
Strath Vaich Dam	0.55	−0.04	69.67	0.56	−0.06	68.31	72.64	324
Aston Hill	0.69	0.02	71.22	0.71	0	69.85	69.92	314
Great Dun Fell	0.46	0.2	68.12	0.48	0.17	67	55.85	362
Harwell	0.64	0.31	66.34	0.65	0.29	65.32	50.83	354
Ladybower Res.	0.75	0.12	65.93	0.75	0.1	64.52	58.83	357
Lullington Heath	0.62	0.22	72.57	0.6	0.21	72.12	59.69	359
Narberth	0.49	0.26	76.52	0.51	0.23	75.05	60.03	267
Auchencorth Moss	0.64	0.14	68.76	0.64	0.11	67.35	60.43	359
Weybourne	0.71	0.07	64.45	0.71	0.05	64.18	60.3	361
St. Osyth	0.63	0.29	69.5	0.59	0.29	69.45	53.91	336
Market Harborough	0.78	0.16	65.77	0.78	0.14	64.6	56.5	365
Lerwick	0.54	0.02	**70.51**	0.5	0	69.03	68.44	356
Eibergen	0.78	0.65	59.75	0.78	0.63	59.58	31.78	357
Kollumerwaard	0.71	0.31	69.08	0.71	0.29	67.94	52.85	348
Vredepeel	0.7	0.51	70.27	0.7	0.49	69.23	46.43	286
Cabauw	0.69	0.56	70.25	0.69	0.54	69.43	44.95	281
De Zilk	0.63	0.49	71.18	0.64	0.48	70.65	47.72	312
Birkenes	0.5	0.2	**65.86**	0.46	0.17	63.97	54.76	353
Prestebakke	0.59	0.13	**64.69**	0.55	0.09	62.66	57.43	365
Sandve	0.62	0.07	**71.36**	0.58	0.03	68.8	66.57	365
Hurdal	0.51	0.06	54.01	0.51	0.04	52.87	50.76	365
Bredkälen	0.46	−0.07	52.69	0.46	−0.09	51.76	56.76	356
Råö	**0.62**	0.13	**69.84**	0.54	0.09	67.35	61.65	365
Norra-Kvill	0.56	0.03	**61.83**	0.5	0	59.99	58.07	365
Grimsö	0.54	0.11	57.86	0.52	0.08	56.42	52.18	365

Table 6. Comparison of simulated NO_3^- concentrations with observations in $\mu g\,m^{-3}$. Values that are significantly different between the base case and the no-ships case are printed in bold.

	base case			no ships			observations	
station	corr	NMB	mean	corr	NMB	mean	mean	# samples
Waldhof	0.71	−0.06	0.22	0.71	−0.16	0.18	0.32	236
Neuglobsow	0.75	0.16	**0.19**	0.75	0.03	0.15	0.3	234
Zingst	0.74	−0.13	**0.24**	0.72	−0.29	0.16	0.45	235
Oak Park	0.84	−0.15	**0.09**	0.82	−0.27	0.07	0.17	255
Malin Head	0.8	−0.31	**0.06**	0.78	−0.4	0.04	0.11	310
Carnsore Point	0.81	−0.38	**0.07**	0.79	−0.47	0.06	0.19	347
Kollumerwaard	0.56	0.07	**0.58**	0.53	−0.07	0.44	0.79	239
Birkenes	0.35	−0.16	**0.05**	0.34	−0.3	0.04	0.1	298
Hurdal	0.26	1.28	0.1	0.26	1.06	0.09	0.07	295

Table 7. Comparison of simulated SO_4^{2-} concentrations with observations in $\mu g\,m^{-3}$. Values that are significantly different between the base case and the no-ships case are printed in bold.

	base case			no ships			observations	
station	corr	NMB	mean	corr	NMB	mean	mean	# samples
Westerland	0.55	−0.04	**0.61**	0.52	−0.14	0.54	0.62	242
Waldhof	0.5	−0.25	**0.56**	0.49	−0.3	0.51	0.7	236
Neuglobsow	0.48	−0.18	**0.54**	0.47	−0.26	0.48	0.64	240
Zingst	0.52	−0.13	**0.6**	0.47	−0.29	0.47	0.64	241
Tange	0.55	−0.04	**0.45**	0.5	−0.13	0.41	0.44	355
Keldsnor	**0.56**	−0.07	**0.6**	0.48	−0.22	0.49	0.61	340
Anholt	0.6	−0.12	**0.48**	0.54	−0.22	0.41	0.53	339
Ulborg	0.45	0.05	**0.54**	0.39	−0.03	0.49	0.48	353
Eskdalemuir	0.43	0.3	**0.39**	0.39	0.18	0.36	0.26	333
Lough Navar	0.29	0.41	**0.38**	0.26	0.3	0.34	0.22	213
Barcombe Mills	0.48	−0.11	**0.59**	0.45	−0.2	0.52	0.59	280
Yarner Wood	0.52	0.03	**0.53**	0.45	−0.11	0.45	0.42	268
High Muffles	0.41	0.32	**0.49**	0.33	0.21	0.45	0.34	232
Oak Park	0.5	−0.02	**0.4**	0.44	−0.11	0.36	0.34	257
Malin Head	0.5	−0.07	**0.44**	0.46	−0.15	0.4	0.44	335
Carnsore Point	0.58	−0.18	**0.5**	0.56	−0.25	0.45	0.58	348
Bilthoven	0.41	0.1	**0.67**	0.39	0.02	0.62	0.51	308
Kollumerwaard	0.37	0.15	**0.59**	0.32	0.05	0.53	0.43	348
Vredepeel	0.35	0.17	**0.7**	0.36	0.11	0.66	0.49	322
De Zilk	0.34	0.29	**0.69**	0.29	0.16	0.62	0.43	351
Birkenes	0.41	0.37	**0.35**	0.35	0.28	0.32	0.2	347
Hurdal	0.21	1.23	0.37	0.18	1.11	0.34	0.15	359
Bredkälen	0.26	0.69	**0.23**	0.24	0.54	0.21	0.12	334
Råö	0.63	−0.21	**0.43**	0.6	−0.28	0.38	0.52	357

Table 8. Annual number of exceedances of the ozone threshold of 120 µg m^{-3}. For the areas represented see Fig. 1.

	Area 1	Area 2	Area 3	Area 4	Area 5
all emissions	9	19	27	46	29
without ships	4	6	14	42	18

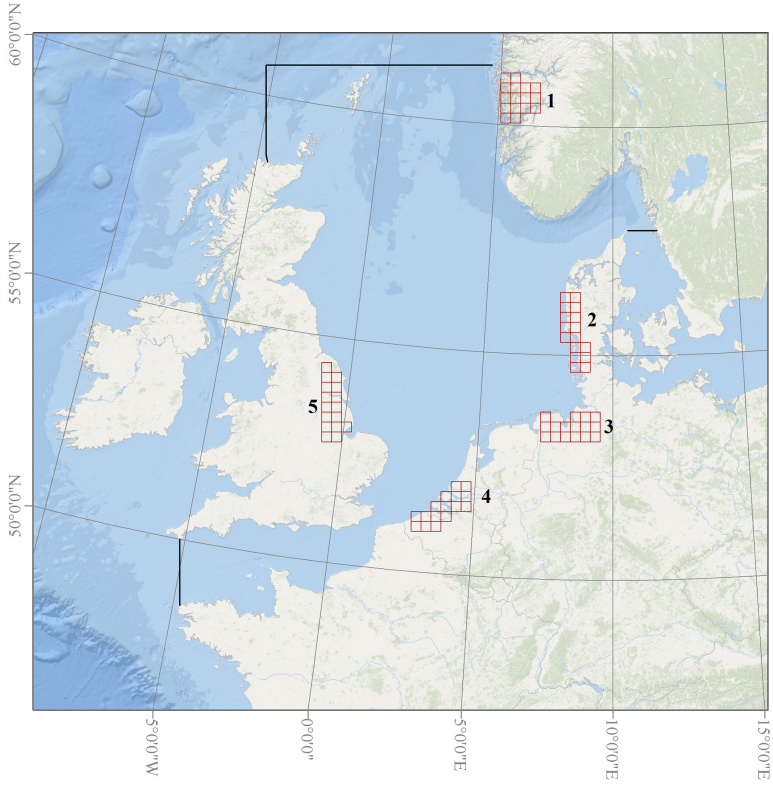

Figure 1. Modeling domain with the borders of the OSPAR region II and the cells that were defined as representative coastal areas.

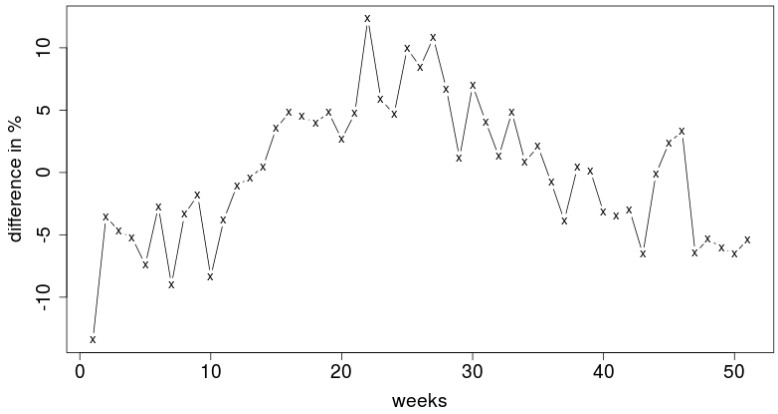

Figure 2. Monthly deviation from the annual mean fuel consumption in the North Sea in %.

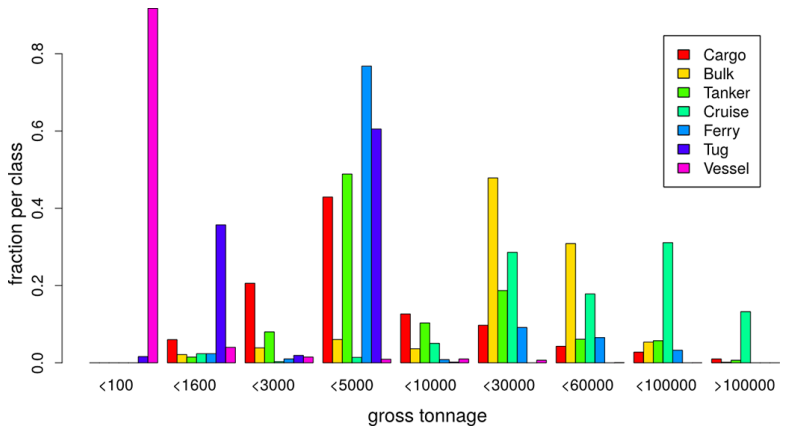

Figure 3. Distribution of ship types across classes.

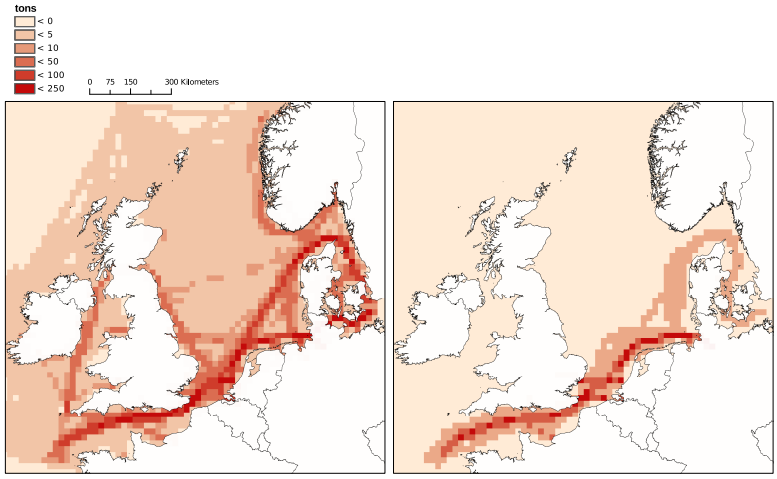

Figure 4. NO_x emissions of cargo ships between 5000 and 10 000 GT (left) and > 100 000 GT (right).

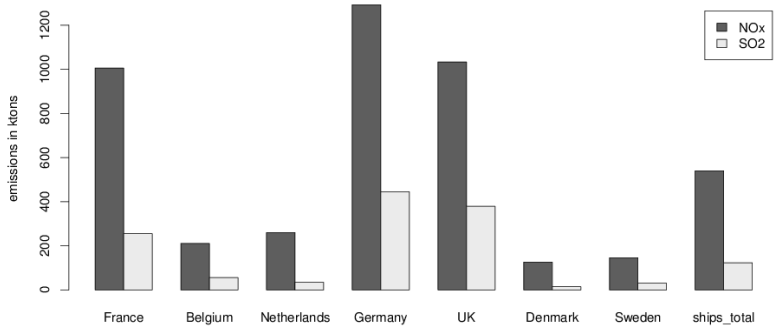

Figure 5. Total NO_x and SO_2 emissions of ships in 2011 compared to some country emissions.

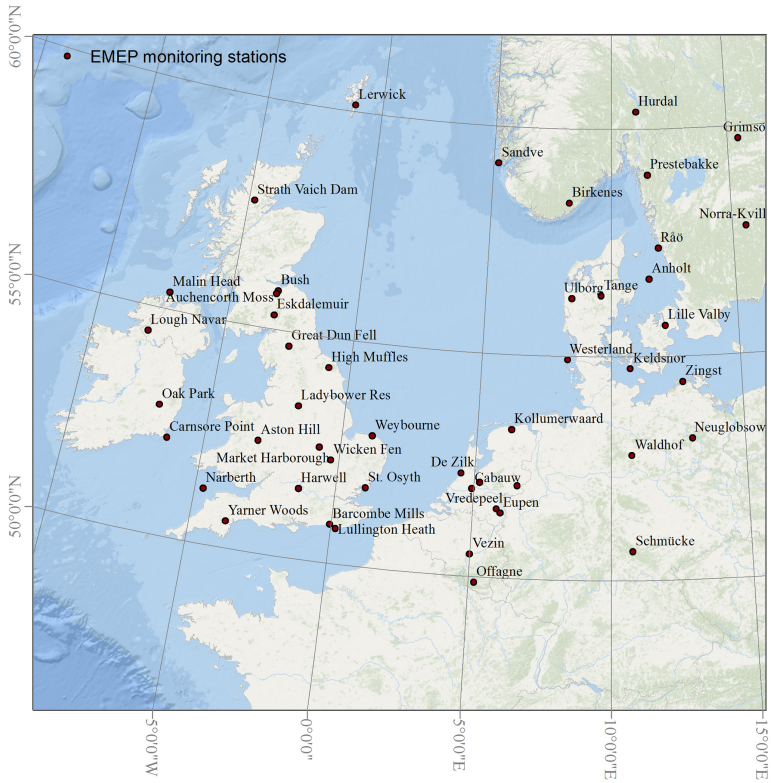

Figure 6. Locations of the EMEP measurement stations used for model evaluation.

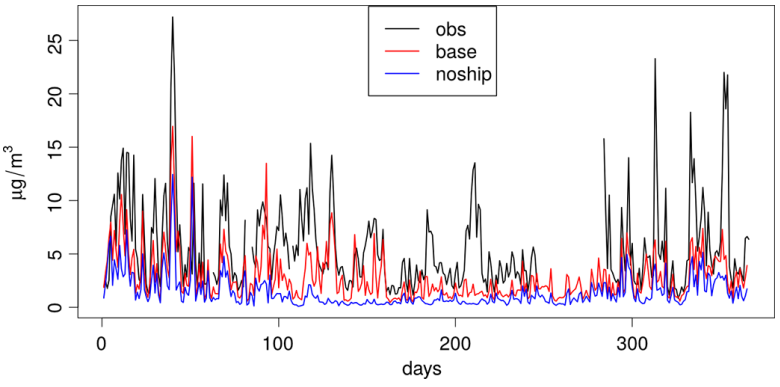

Figure 7. NO_2 concentration time series at Anholt.

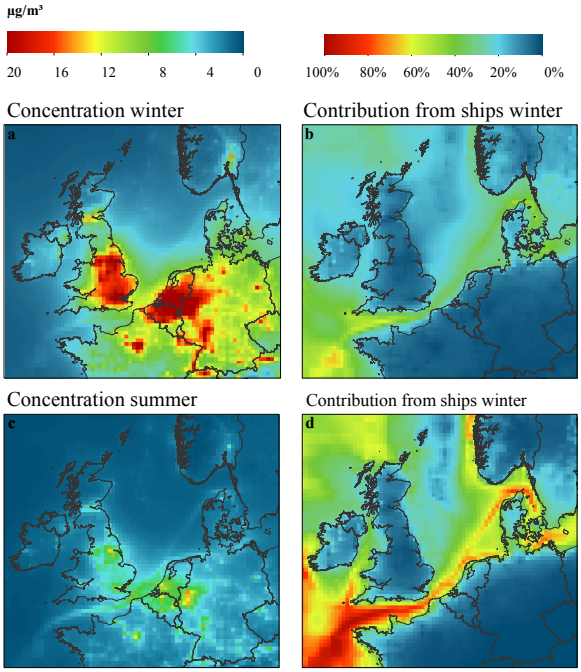

Figure 8. NO_2 in summer and winter and the relative contribution of ship emissions.

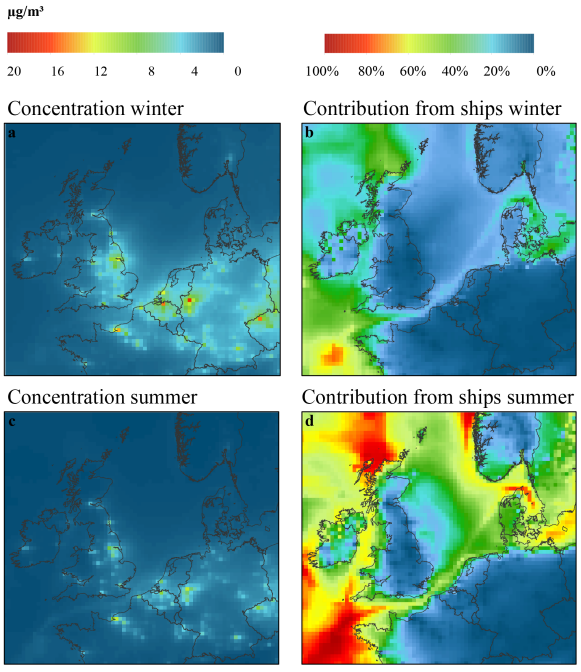

Figure 9. SO_2 in summer and winter and the relative contribution of ship emissions.

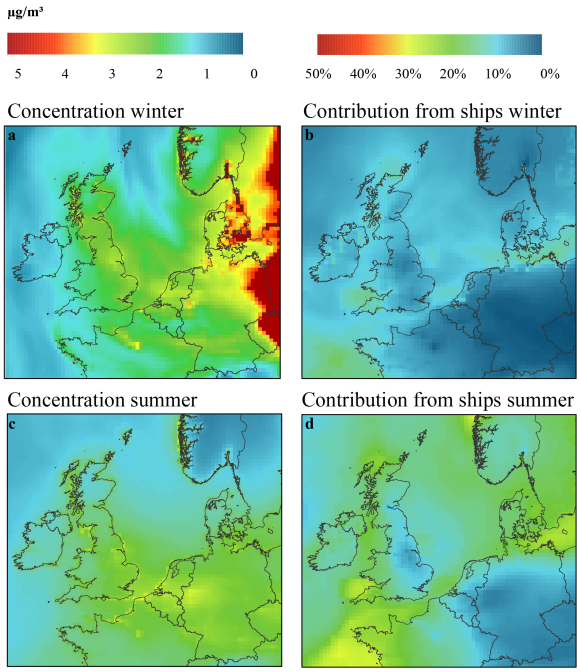

Figure 10. SO_4^{2-} in summer and winter and the relative contribution of ship emissions.

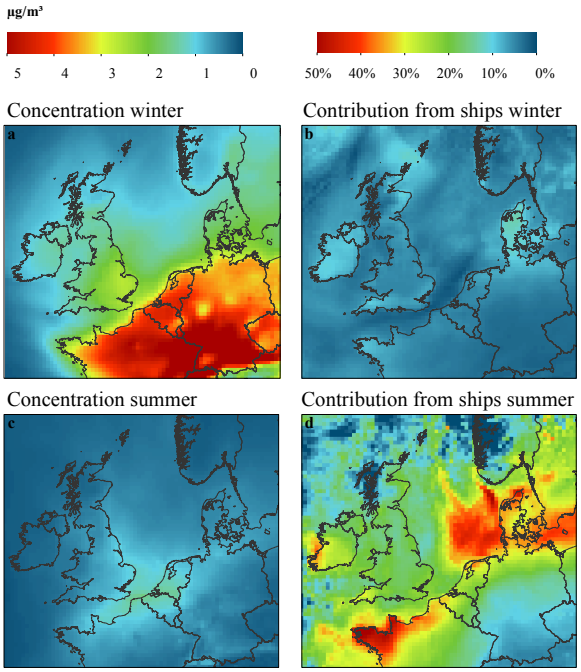

Figure 11. NO_3^- in summer and winter and the relative contribution of ship emissions.

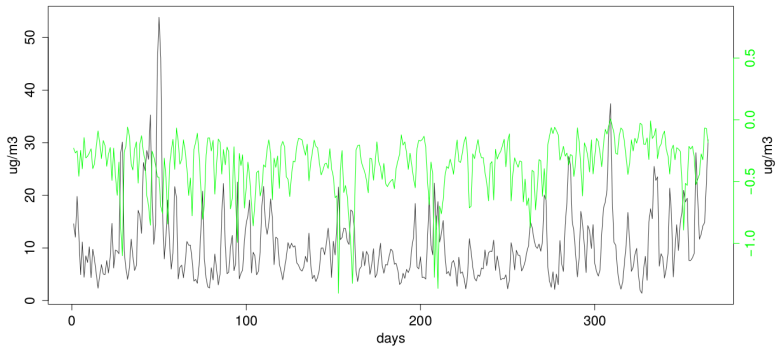

Figure 12. $PM_{2.5}$ time-series. Concentrations averaged over the Dutch and Belgian coast (area 4) and the negative bias if ship emissions were excluded.

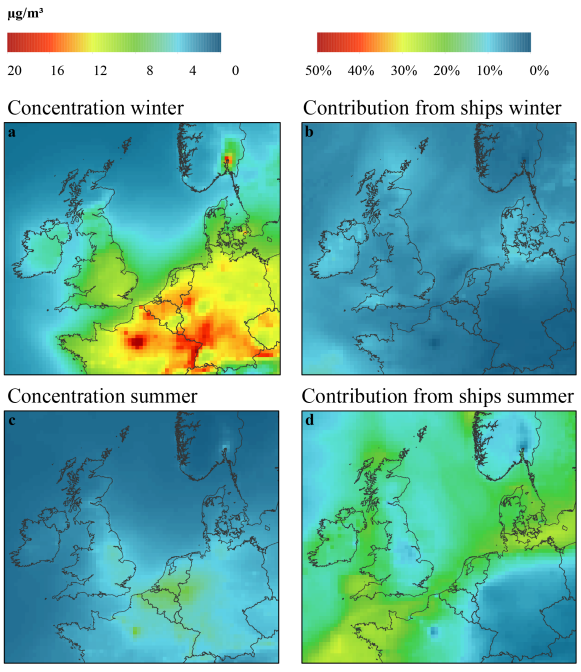

Figure 13. $PM_{2.5}$ in summer and winter and the relative contribution of ship emissions.

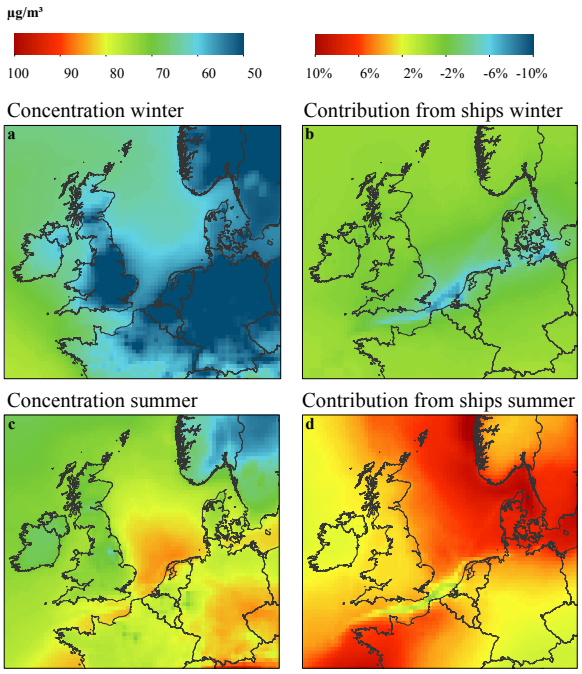

Figure 14. O_3 in summer and winter and the relative contribution of ship emissions.